Hydration of Oxo Anions

A Combined Computational and Experimental Structure and Dynamics Study in Aqueous Solutions

Lars Eklund

Faculty of Natural Resources and Agricultural Sciences
Department of Chemistry and Biotechnology
Uppsala

Doctoral Thesis
Swedish University of Agricultural Sciences
Uppsala 2014

Acta Universitatis agriculturae Sueciae
2014:8

ISSN 1652-6880
ISBN (print version) 978-91-576-7964-2
ISBN (electronic version) 978-91-576-7965-9

Print: SLU Service/Repro, Uppsala 2014

Hydration of Oxo Anions. -A Combined Computational and Experimental Structure and Dynamics Study in Aqueous Solutions

Abstract

The structure and dynamics of several hydrated oxo anions were studied using multiple methodologies. Aqueous solutions of sulfate, sulfite, thiosulfate, peroxysulfate, selenite, selenate, hypochlorite, chlorite, chlorate, perchlorate, bromate, iodate and periodate salts were studied using large angle X-ray scattering (LAXS) and extended X-ray absorption fine structure (EXAFS) spectroscopy. The thiosulfate, selenite and selenate salts were also studied using double difference infrared spectroscopy (DDIR). Moreover, the sulfite, sulfate thiosulfate, chlorite, chlorate and perchlorate ions were simulated using quantum mechanical charge field (QMCF). The periodate ion was shown to have only meta configuration in aqueous solution, while both meta and ortho configurations are present in solid state. The studies showed that the anions could be placed in two main groups, one with asymmetric and another with symmetric hydration. In the asymmetric group consisting of sulfite, selenite, chlorite and chlorate ions where the lone electron-pair of the central atom showed substantially weaker interaction with a longer distance to the water molecules near the lone electron-pair than to those near the oxygens bound to the ion. The symmetric group, sulfate, peroxysulfate, selenate, perchlorate, and periodate ions showed a symmetric interaction with one M-(O···H)-O_{aq} distance to the hydrated water molecules. The iodate and bromate ions probably have an asymmetric hydration, but further studies are required to confirm this. The thiosulfate ion is asymmetric but has a predominantly symmetric exchange mechanism where water molecules exchange directly in all directions between the hydration shell and bulk. Considering the number of water molecules interacting with the ion there is a periodic trend of decreasing number of interactions with border-line between series 3 and 4, which was evident for all ions studied. The hypochlorite ion is a special case as it has a coordination similar to that of the chloride ion. The hypochlorite ion hydrogen binds eight water molecules with five to chlorine and three to oxygen. The results led to the conclusion that when the ion was asymmetric the lone electron-pair effects of the central atom dominated the water exchange mechanism, giving rise to multiple distances and an angular dependence of the exchange between the hydration shell and the bulk water. This effect is prominent for the structure making ions, such as the sulfite ion, and to a lesser degree in the structure breaking oxochloro anions, which have a much higher degree of disorder and significantly less effects from the difference in electron density across the ion.

Keywords: hydration,oxoanion,coordination, QMCF/MD, LAXS, EXSAFS, DDIR, simulation

Author's address: Lars Eklund, SLU, Department of Chemistry and Biotechnology, P.O. Box 7015,750 07 Uppsala, Sweden

E-mail: Lars.Eklund@ slu.se

Dedication

To my sons Teomer and Leopold, you brighten my days.

Why make something simple and efficient, when you can make it complex and wonderful.

By Unknown

Contents

List of Publications

This thesis is based on the work contained in the following papers, referred to by Roman numerals in the text:

I Lars Eklund , Thomas S. Hofer , Andreas B. Pribil , Bernd M. Rode and Ingmar Persson(2012). On the Structure and Dynamics of the Hydrated Sulfite Ion in Aqueous Solution – An ab initio QMCF MD Simulation and Large Angle X-ray Scattering Study, Dalton Trans., 2012, 41 (17), 5209 - 5216.

II Lars Eklund, Ingmar Persson. Structure and hydrogen bonding of the hydrated selenite and selenate ions in aqueous solution, Dalton Trans., 2014, 43 (17), 6315 - 6321.

III Lars Eklund, Thomas S. Hofer, Alexander K. H Weiss, Andreas O. Tirler and Ingmar Persson. Detailed structure elucidation of the hydrated thiosulfate ion using QMCF MD simulation and large angle X-ray scattering in aqueous solution, (Manuscript)

IV Lars Eklund, Thomas S. Hofer and Ingmar Persson Structure and water exchange dynamics of hydrated oxo halo ions in aqueous solution using QMCF MD simulation, large angle X-ray scattering and EXAFS, (Manuscript)

The contribution of Lars Eklund to the papers included in this thesis was as follows:

I All computational work up, except sulfate ARD in collaboration with Thomas Hofer and Andreas Pribili, participated in the collection and data treatment of the X-ray data and major contributions to the text

II All IR work, participated in the collection and data treatment of the X-ray data and major contributor to the text

III Computational work up and analysis in collaboration with Thomas Hofer and Alexander Weiss, participated in the collection and data treatment of the X-ray data, contributor to the text

IV Computational work up and analysis in collaboration with Thomas Hofer, participated in the collection and data treatment of the X-ray data, contributor to the text

Abbreviations

ARD	Angular radial distribution function
DDIR	Double difference infrared spectroscopy
LAXS	Large angle X-ray scattering:
EXAFS	Extended X-ray absorption fine structure
QMCF	Quantum molecular charge field
MD	Molecular dynamics
MRT	Mean residence time
FTIR	Fourier transformed infrared spectroscopy
RDF	Radial distribution function
fwhh	Full width half height

1 Introduction

1.1 Background

The hydration of ions has been studied for a long time, because of the impact it has on the properties of solutions used both in industry and in nature. When the project that this thesis describes started in 2008, the aim was to investigate the hydration of some oxo-anions of group 16 and 17. The project was started with structural studies using large angle X-ray scattering (LAXS) and double difference IR (DDIR). Early into the project, it was expanded to include computer simulation in collaboration with the University of Innsbruck, Austria. This allowed studies of dynamics of the hydration shell as these systems with weak interactions have too high mobility to have the dynamics investigated by experimental methods. This has enabled a unique combination of structural studies in solution through LAXS, DDIR and X-ray absorption spectroscopy (XAS) and computer simulations, which led to the discovery of the asymmetric dynamics of the hydration of some oxo-anions and the difference compared to other more symmetric systems.

1.2 Aim

At the start of the project a number of anions were investigated to find systems that were suitable to go forward with to study the hydration and dynamics of anions in solution as part of a larger project funded by the Swedish Research Council investigating the properties of hydrated anions in aqueous solutions. The anions selected for the project became sulfite, SO_3^{2-}, in paper I, selenite, SeO_3^{2-}, and selenate, SeO_4^{2-}, in paper II, thiosulfate, $S_2O_3^{2-}$, in paper III and hypochlorite, ClO^-, chlorite, ClO_2^-, chlorate, ClO_3^-, perchlorate, ClO_4^-, bromate BrO_3^-, iodate IO_3^- and periodate IO_4^- in paper IV. The oxosulfur and -chloro ions were studied with regards to hydration structure and hydration dynamics

with the aim to elucidate the properties of the hydrated solutions with regards to oxidation state of the anion, transport mechanisms of water molecules in the hydration shells and whether the ion fits into the concept of structure maker or breaker. The rest of the ions were only studied in respects to their structure in comparisons with the oxosulfur and -chloro anions

1.3 Hydration: forces, models and modes of interaction

In inorganic and physical chemistry, hydration can be used to describe the state of an ion in an aqueous solution. The most abundant interaction in aqueous solutions is the electrostatic interaction classified as hydrogen bonds between the water molecules. The solute also interacts with the water through electrostatic interactions typically ranging from strong hydrogen bonds to fairly weak interactions. The water molecules directly interacting with the solute is called the first hydration sphere, those water molecules interacting with water molecules in the first hydration sphere define the second one and so on until the interactions are not distinguishable from bulk water. If the interactions are stronger than bulk water the solute is defined as a structure maker (Gurney, 1953; Marcus, 1994, 2009) and if these are weaker than in bulk water as a structure breaker. The hydrogen bonding is what gives aqueous solutions and pure water many of their physical and chemical properties. The recommended definition of the hydrogen bond is "an attractive interaction between a hydrogen atom from a molecule or a molecular fragment X–H in which X is more electronegative than H, and an atom or a group of atoms in the same or a different molecule, in which there is evidence of bond formation." (Arunan *et al.*, 2011). This definition refers to an electrostatic interaction between two molecules where one of the molecules has hydrogen acting as a charge transfer bridge between them. The bond angle X-H···Y is close to 180° and the strength of the bond increases with increasing linearity of the bond. When analysing the hydrogen bond status there will be a distribution of the bond angle and distance as temperature increase from zero Kelvin, which must then be accounted for. I have therefore allowed for hydrogen bond angles spanning 35 degrees from linear the (0° or 180°) axis along the bond when analysing the simulation data. The distance criteria allowed for a hydrogen bond is much more difficult to address as it changes depending on acceptor-donor pair and has to be estimated from the occupied distances of a given system. The hydrogen bonds present in the systems described in this thesis are near the strength of the bulk water interactions in pure water.

1.4 Oxidation number

Oxidation number (ON) is a convenient way to describe oxidation and reduction reactions based on a set of commonly agreed upon rules. It is the charge an atom would have if all ligands and all electron pairs shared with those ligands were removed. It is not an indication of electron distribution across a polyatomic coordination entity. This of course reduces its usefulness in assessing the effects an ion has on its surrounding, and oxidation number or state have little influence on the hydration of these entities.

1.5 Difference between pure water and aqueous solutions

When studying aqueous solutions using multiple experimental methods and theoretical models studied through simulation, it is important to recognize that the effects of the differences in interactions occurring in an electrolyte solution and pure water can be dramatic. The properties of bulk water in these systems have minor but significant differences largely depending on the charge density of the electrolyte ions. The systems that I have studied have minor effects of such type because they have a low charge density and therefore affect order less. Nevertheless, it is important to note that only systems where the direct influence from the counter ion on molecules in the hydration sphere is negligible, should be studied with simulations using no counter ions. For these simulations, it is of importance that the charge field is constructed in such a way that it does not influence the properties of bulk water as a counter ion does, but rather shields the ion of interest from self-interactions. In a concentrated electrolyte solution, such effects are expected to be large and decreasing as distance between ions increase when the solution is diluted. If the electrolyte has low charge density such as perchlorate, sodium or oxosulfur ion the interactions with counter ions is much lessened and the solution approaches the situation of the theoretical charge field approach which gives a pure water like solution as used in simulation. On the other hand, it is significant in systems like the magnesium ion, which is an ion with high charge density. As I study solvated electrolytes with weak interactions giving solutions close to what could be called an electrolyte solution with pure water properties the former case applies. However, there might be a difference between the physical solution and that of the simulation, which causes a divergence when studying the exact strength of the hydrogen bond in comparison to bulk water bonds. The pure water-like bond structure of the bulk in simulation might differ from structure determined by experimental methods that may have electrolyte affected bulk water to a greater extent than that seen in simulation. These effects are concentration-dependent influences generated by the solvated ions.

1.6 Symmetry of hydration shells

When considering the hydration of more complex systems such as poly-atomic ions, which may have interactions that differ across the ion, how symmetric the hydration "sphere" is differs from simple atomic ions. It is quite common to see cases that differ quite signif-icantly from a spherical system where the dyn-amics of water exchange at different sites are affected. This observation coincides with the observation that ions such as SO_3^{2-} reacts more commonly where the weaker interaction with the hydrated water are which is also the site of exchange of the water molecules in the first sphere with those outside of the first hydration sphere. In the symmetrical shell, we expect to see an even distribution of structure and dynamics. Earlier studies on sulfate (Vchirawongkwin *et al.*, 2007) and perchlorate (Lindqvist-Reis *et al.*, 1998) demonstrate these effects. When dealing with asymmetric systems a more appropriate term to use could be hydration shell as it is less misleading than the inherently symmetrical term hydration sphere. A hydration shell is therefore best described by which atoms are interacting see figure 1. Thus, the first hydration shell is defined as those water molecules that interact directly with the solute, the second is the water molecules that interact with waters in the first hydration shell and the third and higher shells are those that interact with the water molecules in the previous shell. The hydration shells get defined in increasing numeration until one has a shell that has interactions that are indistinguishable from the previous step and any following steps, which then become labeled as bulk water.

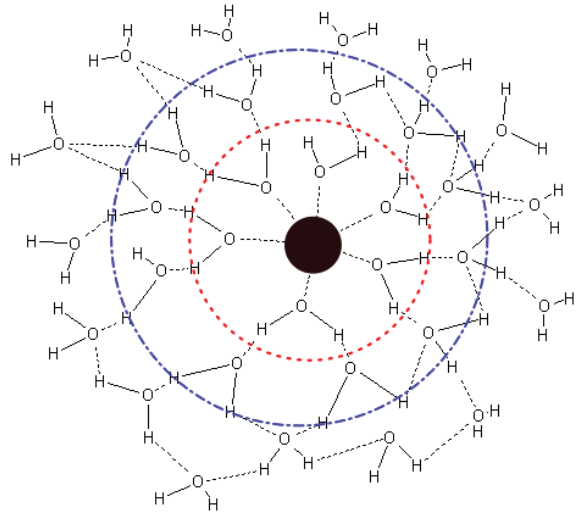

Figure 1. Schematic picture of a coordination entity (filled circle) and its first two hydration shells. In the first shell, marked by a red dotted circle, the water molecules interact directly with the coordination entity. In the second shell enclosed in a blue dash-dot circle the water molecules hydrogen bind to the water molecules in the first.

1.7 Anionic hydration

Hydrogen bonding and other electrostatic interactions with properties that are hydrogen bond-like dominate the anionic hydration. Whether the interaction is weaker or stronger in nature, it is always bridged by the hydrogen in water, binding the ion to the surrounding waters with columbic interactions. For monovalent monoatomic anions the hydration is well studied (Ohtaki & Radnai, 1993) and behaves closely to that of the metallic cations, but for polyatomic anions the hydration becomes more complex as the charge is no longer uniformly distributed. The effects of shielding become quite noticeable and the interactions with the surrounding water becomes much more complex. When studying the anionic system it is important to remember that the water molecules and the solute may be influenced by the cationic counter ion. This is why comparison with simulation where no counter ion influences are present gives substantially more information than experiment or simulation alone.

2 Methods

2.1 Quantum mechanical charge field/molecular dynamics

The quantum mechanical charge field/molecular dynamics (QMCF/MD) (Rode & Hofer, 2006; Rode *et al.*, 2006) is a combination of quantum mechanical (QM) calculation around the solute and an outer layer of molecular mechanics (MM) calculation. The simulation box is thereby partitioned into three regions see figure2. The force equation on a particle J therefore has different functions depending on if the molecule is in the core region closest to the solute F_J^{core} or in the bulk region calculated by MM F_J^{MM}. This approach avoids surface artifacts from calculation in artificial vacuum by including point charges from the MM region into the QM force equation. A reaction field approach, charged field, accounts for surrounding media beyond the cutoff radius and core. The equation becomes

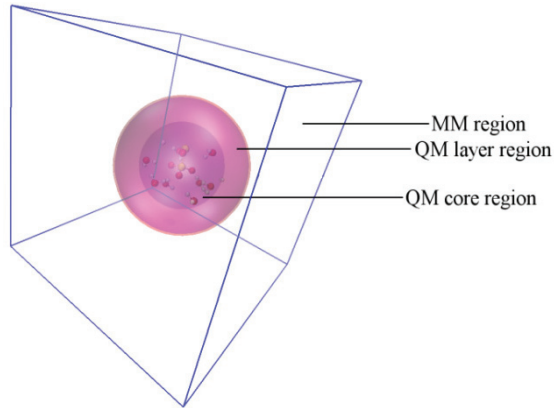

Figure 2. The simulation box is split into two major regions, one quantum mechanic, QM, (spheres) and the rest a molecular mechanic, MM, region. The QM region is further split into a core region (inner sphere) and a layer region (outer sphere). The core region contains the ion of interest and one full hydration sphere and the layer region contains only solvent molecules. At the outermost regions of the QM layer, there is a small smoothing region to handle the transition from QM forces to MM forces.

$$F_J^{core} = F_J^{QM} + \sum_{I=1}^{M} \frac{q_J^{QM} \cdot q_I^{MM}}{r_{IJ}^2} \cdot \left[1 + 2 \cdot \frac{\varepsilon + 1}{2\varepsilon - 1} \cdot \left(\frac{r_{IJ}}{r_c}\right)^3\right]$$

The force equation for the MM region

$$F_J^{MM} = \sum_{\substack{I=1 \\ I \neq J}}^{M} F_{IJ}^{MM} + \sum_{I=1}^{N_1+N_2} \left\{\frac{q_I^{QM} \cdot q_J^{MM}}{r_{IJ}^2} \cdot \left[1 + 2\frac{\varepsilon + 1}{2\varepsilon - 1}\left(\frac{r_{IJ}}{r_c}\right)^3\right]\right\} + \sum_{I=1}^{N_2} F_{IJ}^{nC}$$

A layer is introduced between pure QM region and pure MM region where the force equations for each molecule is calculated both using QM, MM and a smoothing function:

$$F_J^{smooth} = S(r) \cdot \left(F_J^{layer} - F_J^{MM}\right) + F_J^{MM}$$

where $S(r)$ is a continuous function defined as

$$S(r) = 1, r_0 \leq r_1$$

$$S(r) = \frac{(r_0^2 - r^2)^2(r_0^2 + 2r^2 - 3r_1^2)}{(r_0^2 - r_1^2)^3}, r_1 < r < r_0$$

$$S(r) = 0, r > r_0$$

The smoothing function is introduced to ensure that the momentum of the molecule is preserved in the transition from the QM region to the MM region.

When setting the starting conditions of the simulation, many things need to be taken into account. The number of water molecules present must be large enough to give both full hydration and bulk behaviour. The box length needs to be large enough to include any relevant features inside the box and the radius of the QM sphere needs to be large enough to fully include all the hydration shells of interest, including any features of an asymmetric shell. If the radius is placed in such a way that it cuts a region of interest, the affected molecules display artefacts with regards to structural properties etc. Another important factor to consider is the QM diameter to box length ratio, the QM diameter should not be in excess of half of the box length. If the QM diameter is longer, the edge particles will interact with directed forces, which will cancel out. The scale of this problem is of course dependent on population size in the edge region and may be negligible in some systems where weak interactions

between the particles are expected at the distance of the edge and which has a low population density at the edge region.

2.2 X-ray based methods

2.2.1 Large angle X-ray scattering

The large angle X-ray scattering (LAXS) method uses that electrons scatter X-ray radiation to calculate the inter-atomic distances in the sample. This method has been used for a long time and is well detailed elsewhere (Persson, 1984), here follows a short summary of the technique. An X-ray beam is directed onto the sample and when the X-ray beam encounters electrons in the sample it may scatter. The intensity of the scattering is measured at different angles using a Θ-Θ goniometer.

$$I/N = I_{eu} + R\sum i(c)$$

The intensity function is dependent on two parts of scattering, coherent and incoherent. The coherent scattering I_{eu} is calculated using atomic form factors,

$$I_{eu} = \sum_m \sum_n f_m f_n \frac{\sin sr_{mn}}{sr_{mn}}$$

where s is $s = 4\pi \sin\theta/\lambda$, r is distances between atoms m and n, f is the atomic form factors taken as tabulated (Prince, 2006), which are calculated at the Hartree Fock (HF) level of theory.
By subtracting the form factor for the free electron radial density,
the intensity function can be transformed into structural information.

$$f_e = \int_0^\infty 4\pi r^2 \rho(r) \frac{\sin sr}{sr} dr$$

In my experiments I used scattering Mo K_α X-ray radiation with a wavelength of λ=0.7107 Å. To get monochromatic radiation a LiF(200) single crystal was used and the scattering was determined at about 450 angles in the angle range of Θ between 0.5º to 65º. To achieve a good statistical error in the intensity, about 0.3 %, 100,000 X-ray quanta were collected at each angle and the entire range was scanned at least twice. The divergence of the beam was defined through a set of divergence-collecting focal slits of ¼º-½º-0.2 mm and 1º-2º-0.2 mm. All data was processed using the KURVLR program (Johansson & Sandström, 1973) and the structural parameters in the theoretical model were refined by minimizing $U = w(s)\Sigma s^2[i_{exp}(s)-i_{calc}(s)]^2$ using the STEPLR program (Chandler, J. P., 1969; Molund & Persson, 1985). Furthermore one

has to normalize to a stoichiometric unit containing one atom of interest in order to get a simple interpretation and computationally easier model, by using the scattering factors *f* for neutral atoms, including corrections for anomalous dispersion, $\Delta f'$ and $\Delta f''$ (Prince, 2006), Compton scattering (Cromer, 1967, 1969) and multiple scattering events. In the cases I have studied the latter is especially important. With these systems where the molar absorption coefficients μ of the solutions was low below 10 cm^{-1} and therefore the penetration of the X-ray into the sample is high, generating significant effects from multiple scattering

2.2.2 X-ray absorption spectroscopy

X-ray absorption spectroscopy (XAS) is based on absorption or fluorescence of X-rays preferably generated from a synchrotron radiation source. For a detailed description on XAS see the thesis by Jalilehvand (Jalilehvand, 2000) is suggested. In this thesis only a brief overview of the subject will be covered and focusing on the absorption spectra. XAS phenomenon is brought about when X-rays hit the electrons with sufficient energy to excite an inner core electron, giving rise to a core hole. Depending on the chemical environment, wave interference during the core-hole lifetime will give rise to intensity variations of the resulting photon release when the core hole is populated again. These energy dependent variations can be used to analyse the environment close to the absorber

X-ray Absorption Fine Structure

The region of the X-ray absorption spectrum called the extended X-ray absorption fine structure (EXAFS) region gives information about the nearest neighbour atoms surrounding the absorbing atom. The region is considered from 50 eV to >1000 eV above the absorption edge. By fitting theoretical scattering paths to the intensity function one can through Fourier transformation generate a radial distribution function. The distances represent the distance travelled by the photoelectron wave. The near edge X-ray absorption fine structure (NEXAFS) region extends from a few eV from the edge to about 50 eV above the edge. It can give information about the coordination geometry around the absorbing atom.

X-ray absorption near edge structure

X-ray absorption near edge structure (XANES) extends to about +-10 eV around the main absorption edge. At the peak of the absorption edge there is sometimes a sharp and intense increase in absorption, a so-called white line. This is due to the transition of an electron to an energy level close to the

continuum; these energy levels are closely spaced, and therefore have a high probability of becoming populated when an X-ray excites the absorber. The position of the white line absorption is influenced by the oxidation state of the absorber because of changes in the potential energy between electrons and the core. The increase in potential energy as the oxidation state increases means an increase in energy with about 2 to 8 eV. Features around the edge such as minor peaks and valleys arise from the coordination geometry as it affects the energy level of the valence shell.

2.3 Double Difference Fourier Transformed Infrared Spectroscopy

Double difference Fourier transformed infrared spectroscopy (DDFTIR) also commonly referred to as double difference infrared spectroscopy (DDIR) was first developed by Kristiansson and Lindgren (Kristiansson *et al.*, 1988). The inclusion of Fourier transformation has enabled the use of modern spectroscopic instruments, but it is essentially the same as the DDIR technique and will be used analogously in this text. The essentials of the technique is that one probes the O-D stretching frequency change for spectroscopically identifiable water molecules in the hydration shell, using the difference between the spectra of 8% HDO Solutions with corresponding spectra in pure water. The affected water peaks ascribed to water molecules bound to cations or anions can be evaluated. This is achieved by taking the derivative of these spectra ϭϵ/ϭm where ϵ is the spectra and m the molality of the solution. Then subtract (1/*N***M*)*ϭϵ/ϭm from the spectrum of pure water, where *N* is the affected number of water and M is the mean molar mass in kg/mol of water and partially heavy water. Finally, the peaks can be evaluated using principal component analysis. This is described by Kristiansson (Kristiansson *et al.*, 1988). and Gampe (Stangret & Gampe, 1999, 2002). All calculations of the spectra was carried out using GRAMS AI version 8.0 (Thermo-Fisher Scientific) and RAZOR tools (Spectrum Square Associates), and the ArrayBasic programs YANUZ.AB and PROBABIL.AB (Smiechowski)was used to calculate derivatives of spectra.

2.4 Literature review and structure database search

In all structural work experimental as well as computational simulation, it is paramount to find a good starting position for the initial models. These are typically found in structural databases which is the approach applied in all the papers included in this thesis. The databases utilized were FIZ/NIST Inorganic

Crystal Structure Database (Belsky *et al.*, 2002; Bergerhoff, G. & Brown, I.D., 1987)and Cambridge Structural Database(CSD)(Allen, 2002). When selecting which structures to include it is important to check that one does not use a structure where the counter ion to the ion of interest deforms the electron cloud to a large extent. Preferably, it should be a large ion with low charge density such as sodium. The sodium ion has been shown to not influence the hydration shell of the ion of interest. To make a complete average of the structures found most which are in solid crystalline state, it is important to include as many structures as one can find that are chemically similar and which do not perturb the electron cloud to a large extend. When the average distance is found, compensation in the initial method must be made to take into account that hydrogen bonds formed in solution will increase the intra molecular bond distance by drawing out the electrons. The difference between a crystal and solvated ion is about 0.2 Å elongations of the intra molecular distances.

2.5 Methods of data analysis

The analysis of QMCF/MD simulations was done using a number of tools. The radial density function g(r) is an atomic population function across a radial distance from a given central atom. All atoms are considered point wise and in contrast to the experimental radial distribution function, RDF, where the background, $4\pi r^2\rho_0$, is subtracted one it is normalized to the same. In the analysis of the experimental data, one assumes that where there is a coalescence of electrons there is an atom present.

From simulation data it is possible to make a conical selection of the radial distribution function thereby generating g(r,α) which is then repeated around the molecule of interest generating a sun ray pattern of the averaged cone values which are then interpolated to give the angular radial density function, ARD.

By plotting radial distance and angle for a selected number of water molecules one can study the possible pathways a given water molecule takes which may give stronger information on a given region of the ARD.

Another radial tool is mean ligand residence time, MRT. By defining, an inner and an outer cutoff around the hydration peak the direct measurements of exchange events across either boundary can be made. Setting a duration criteria of $t \geq 0.5$ ps where t is the duration between crossing events for a given target atom gives the MRT as $t_{0.5} = CN_{\mathrm{av}} \cdot N_{\mathrm{ex}\,0.5}/t_{\mathrm{sim}}$ where CN_{av} is the average coordination number and t_{sim} is the total simulation time. The ratio of exchanges R_{ex} is obtained by the quotation of $N_{ex\,0.5}$ and the total of all

occurring border crossings, $N_{ex\ 0.0}$, which corresponds to the average number of border crossings needed to achieve one lasting exchange event.

The hydrogen bond correlation functions continuous, $S_{HB}(t)$, and intermittent, $C_{HB}(t)$, are defined as:

$$S_{HB}(t) = \frac{< H(0)H(t) >}{< H >}$$

$$C_{HB}(t) = \frac{< h(0)h(t) >}{< h >}$$

where h(0) is the hydrogen bond population at time zero and h(t) the corresponding population at time t and H(0) and H(t) are analogous but not allowing for reformation of the hydrogen bond. These populations are a time average over the time t. To get the population we define the hydrogen bond depending on distance and angle between the X···H-O where X is the acceptor and O is the oxygen of water. Because the solution will have thermal movement the hydrogen bond angle is allowed to deviate from the ideal 0/180° with 35°. The distance criteria must be adjusted depending on the acceptor as the average hydrogen bond distance is dependent on the acceptor. By fitting the data for $S(t)$ and $C(t)$ with a two part exponential decay:

$$S_{HB}(\tau) = a_0 e^{-t/\tau_1} + (1 - a_0) e^{-t/\tau_2}$$

For the $S(t)$ the short and a long component, τ_1 and τ_2, where the long parameter is the larger of the two, the long parameter corresponds the average hydrogen bond lifetime.

3 Results

3.1 Oxosulfur anions

3.1.1 Sulfite ion

Radial distribution functions from the QMCF/MD simulation determine the structural parameters for the proximal water molecules outside of the oxygens, and the distal water molecules outside of the lone-pair of sulfur. The distances were determined to 3.73 and 4.11 Å, respectively. The full width half height, fwhh, of the peaks was 0.530 and 0.370 Å. The assembly of atoms over the range in the simulation causes the peak width, which corresponds to the thermal broadening of an experimental curve. There is also a broadening of the peaks caused by the influence of long range S···H and O···H interactions. Investigating the details of the S···H RDF there are three average distances that hydrogens of hydrated waters occupy. These correspond to two distances of proximal hydrogens at 2.79 and 4.11 Å and one at 2.99 Å at the distal side. By separating the water oxygens interacting with water, $O_w \cdots O_w$, from the waters interacting with the oxygens of sulfite, $O_{SO3} \cdots O_w$, one get an average distance of 2.83 and 2.77 Å, respectively. The QMCF simulation results are for an ideal solution with no counter ions and only small contributions of the distances come from hydration of the ion, about one in every 300, and as one increases the concentration towards those used in LAXS experiments the hydration shell distances become significant in comparison to bulk. The difference in the intermolecular distance between bulk water oxygens and oxygens of waters hydrating the ion is 0.06 Å, which is consistent with and confirmed by geometries and distances obtained in the analysis of the LAXS data. In Table 1 the comparable distances between simulation and experiment have been compiled. The angular density function, Figure 3, showed low density in the region outside of the oxygens bound to sulfur and an increased density outside of the lone electron-pair. The hydration shell has prominent peaks of higher

density of oxygen atoms near the oxygens and a smaller band along the molecule with another peak near the symmetry axis and the lone electron-pair.

An MRT analysis was done with centering on the sulfur atom, showing that the MRT of the sulfite ion was 3.2 ps. Thus, the sulfite ion has 1.9 times longer mean ligand residence time than that of bulk water which is 1.7 ps (Frisch *et al.*). The symmetric approach used in MRT is not well suited to describe the dynamics of the sulfite ion, as the exchange event is not distributed evenly along the hydration shell as shown by the distance *versus* angle plot and the angular radial distribution functions. This means that the intra shell exchanges are not included in a MRT analysis. It does however give an indication to structure making and breaking properties which is in accordance with earlier publications (Marcus, 1994, 2009).

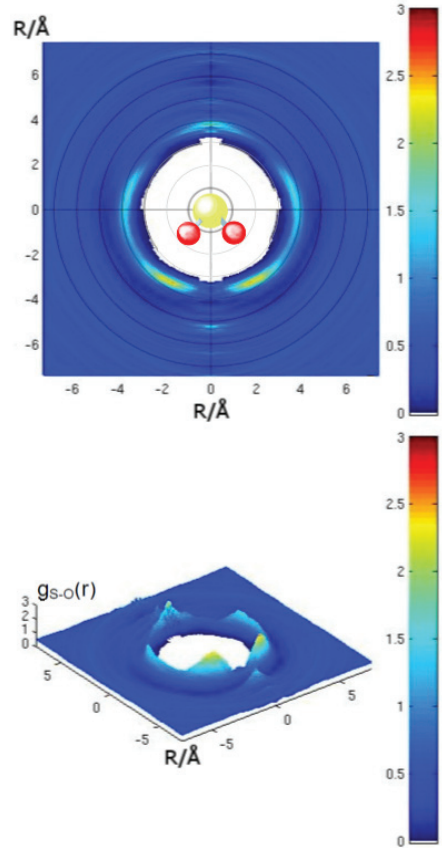

Figure 3. The Angular radial distribution function of sulfite. RDFs are constructed using a conical angle of 18° and the resulting RDFs are interpolated over a 1000 by 1000 grid. The top picture shows the ARD with a top down view and the bottom at viewing angle of 35°, Both are color mapped on $g_{S\text{-}O}(r)$. A clear asymmetry in the occupation outside the first hydration shell can be observed. This indicates that the water exchange only occurs at the lone pair coordinated waters, as these water molecules binds much weaker than those coordinated on the oxygen side.

The sulfite ion has an asymmetric hydration as shown by both experiments and QMCF/MD modeling (Paper I). The structural data included in Table 1 clearly show two distinct distances with a shorter distance of around 3.7 Å for the on average 9 water molecules coordinated to the sulfite oxygens and for the on average 3 water molecules clustered outside the lone pair at about 4.2 Å. This asymmetry was also shown in the angular radial function which showed a clear asymmetry of the hydration Figure 3, seen as a minima just outside the hydration shell near the oxygens which is not present outside the lone electron-pair. This feature hints of a

hydration mechanism that is asymmetric, which was confirmed by an angle distance plot.

3.1.2 Thiosulfate ion, symmetric dynamics with asymmetric structure

LAXS studies and QMCF/MD studies have shown that the water molecules of the hydration shell occupies two average distances, one around the oxygens and one around the terminal sulfur relative to the thiosulfate ion, 2.854 and 3.24 Å, respectively (Paper III). In comparison with the simulation results, there is no significant difference between the distances when taking into account peak widths as seen from the structural parameters given in Table 1. In the ARD it is seen that the dynamics around the terminal sulfur have much in common with that of the sulfite, with loosely bound oxygens clustered around the sulfur. There are minima occurring outside of the oxygens and a continuous exchange around the terminal sulfur. The symmetry of exchange appears to be a mix of the sulfite and sulfate cases. By doing an atomic MRT, indications of the dynamics of the system can be assessed. The atomic MRT showed an average of 3.62 ps for the hydrating waters around the oxygens and 2.43 ps around the terminal sulfur site with t^*=0.5 ps in both cases. Furthermore, the number of exchanges needed to make a complete lasting exchange event was on average 16.1 around the oxygens and 45.6 around the terminal sulfur. The hydrogen bond structure of the hydrated thiosulfate ion can be further analysed using hydrogen bond correlation functions, $C(t)$ and $S(t)$, Figre 4. By fitting the continuous hydrogen bond correlation function to a double exponential, the hydrogen bond life times for the terminal sulfur was found to be 0.223 ps which was 58% that of the

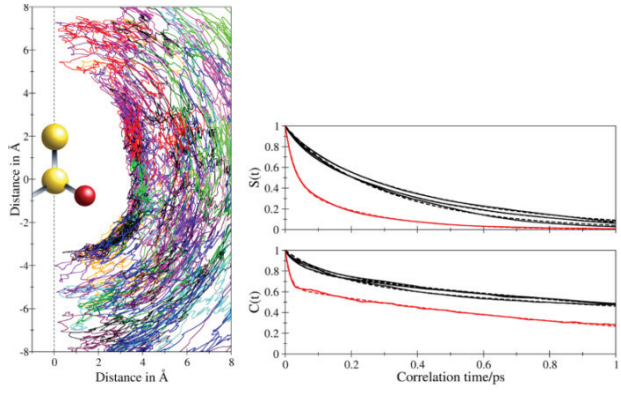

Figure 4. Angle dist-plot showing the pathing of 4 random watermolecules in the hydration shell over the entire simulation(left). The continuous hydrogen bond correlation function S(t) top and the intermitten C(t)(bottom), the oxygen to water hydrogen bonds are in black and the sulfur to water hydrogen bonds are in red. These where fitted to the double exponetial $S_{HB}(\tau) = a_0 e^{-t/\tau_1} + (1 - a_0)e^{-t/\tau_2}$, dashed lines.

oxygens which had an average hydrogen bond life of 0.388 ps. There is a clear indication of asymmetric behaviour in terms of occupancy around the ion and in the life times of the hydrogen bonds. However, as can be seen in the angle distance plot the exchange between the hydration shell and bulk water is not as localized as in sulphite ion hydration but more similar to the sulfate ion. The exchange is increased around the weaker hydrogen bonding structure of the sulfur but not as much as when the coordination voxel is occupied by a lone electron-pair. The results obtained both using MRT and hydrogen bond correlation functions were in contrast to the conclusions presented by Trinapakul et al.(Trinapakul *et al.*, 2013), who reported unexpected results with the terminal thiosulfate sulfur having hydrophobic properties and with an S-S bond distance shorter in aqueous solution than in solid state.

3.1.3 Sulfate ion

To add to the knowledge of the sulfate ion and enable comparison with sulfite an ARD analysis of the sulfate ion, Figure 5, was prepared using simulation data from previously published simulations on sulfate (Vchirawongkwin *et al.*, 2007). This ARD analysis clearly showed that the sulfate has a symmetric hydration shell with a symmetric water exchange around the ion.

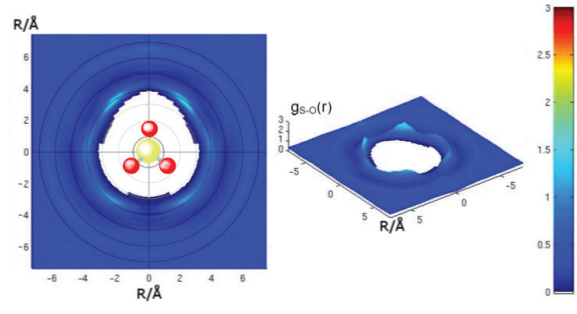

Figure 5. The sulfur oxygen angular radial distribution function, ARD, of the sulfate ion. Using a conical angle of 18°and interpolated over a 1000 by 1000 grid, the left picture shows the ARD with a top down view and the right at viewing angle of 35°. Both are color mapped on $g_{S\text{-}O}(r)$.

3.1.4 Peroxodisulfate ion

The structural determination of peroxodisulfate ion was conducted using LAXS. The structural parameters are given in Table 1. The peroxodisulfate had one discernible distance to the hydration shell, indicating a symmetric hydration of the type found for the sulfate ion. The oxygens of the peroxodisulfate ion has shorter distance to the oxygens of the hydrating water at 2.873 Å as compared to bulk water at 2.89 Å, indicating that it is a weak structure maker like the other studied oxosulfur anions.

Table 1. Structural parameters for the oxosulfur anions as summarized from papers I and III. *N* is the coordinating number as calculated from LAXS measurements, *d* is distance in Å, *b* is the temperature coefficients in $Å^2$, *l* the fwhh. The table's first four columns refer to data from LAXS the last two from simulation data.

Interaction	*N*	*d*	*B*	*l*	*d*	*l*
LAXS					*QMCF MD*	
Sulfite						
S–OSO3		*1.53*		*0.128*	*1.53*	*0.074*
S···Oaq	*9*	*3.68*		*0.219*	*3.73*	*0.530*
S···Oaq,lp	*3*	*4.16*		*0.232*	*4.11*	*0.370*
Oaq···Oaq		*2.878*		*0.210*	*2.828*	*0.299*
Na···Oaq		*2.407*		*0.224*		
O–H					*0.98*	*0.058*
Sulfate						
S-O	*4*	*1.4956*	*0.00272*	*0.0733*		
S···Oaq	*12*	*3.612*	*0.0263*	*0.231*		
Oaq···Oaq	*2*	*2.8801*	*0.02256*	*0.2123*		
$O_{zulf}\cdots O_{aq}$	*3*					
Thiosulfate						
O_{thio}	*3*	*1.479(5)*	*0.0024(5)*	*0.069(7)*	*1.4767*	*0.0330*
S_c-S_T	*1*	*2.9298(6)*	*0.0040(6)*	*0.089(7)*	*2.017*	*0.046*
$O_{thio}\cdots O_{aq}$	*9*	*2.854(1)*	*0.022(2)*	*0.210(2)*	*2.852*	*0.076*
ST···Oaq	*3*	*3.24(5)*	*0.063(9)*	*0.35(3)*	*3.552*	*0.289*
SC···Oaq	*9*	*3.622(7)*	*0.034(2)*	*0.26(1)*	*3.786*	*0.170*
SC···Oaq	*3*	*4.36(6)*	*0.049(7)*	*0.31(2)*	*4.084*	*0.123*
Na-Oaq	*6*	*2.42(2*	*0.0254(8)*	*0.23(1)*		
Oaq···Oaq	*2*	*2.890(2)*	*0.0200(3)*	*0.20(2)*		
Peroxodisulfate ion						
S-Ooxo	*6*	*1.4483*	*0.00273*	*0.0734*		
S-Operoxo	*2*	*1.6746*	*0.00609*	*0.1107*		
Ooxo···Oaq	*3*	*2.8735*	*0.01697*	*0.1844*		
S···Omean	*11*	*3.731*	*0.0201*	*0.201*		
Na-Oaq	*6*	*2.4329*	*0.02459*	*0.2214*		
Oaq···Oaq	*2*	*2.890*	*0.02003*	*0.2002*		

3.2 Oxoseleno anions

The oxoseleno anions where studied by LAXS, EXAFS, XANES and DDIR. The interatomic distances are summarized in Figure 6. Again, dual distances are observed for the hydrated selenite ion while only one distance was present in the hydrated selenate ion. Both are weak structure makers as was shown by the DDIR measurements with a slight redshift of the O-D stretching frequency.

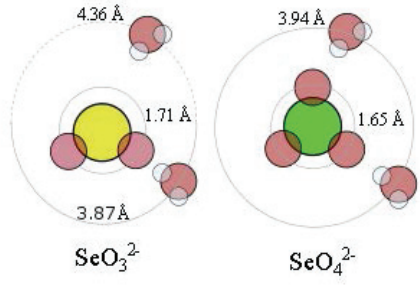

Figure 6. Schematic representation of the hydration distances found in the selenite and selenate ions.

3.2.1 Selenite ion

From LAXS measurements, the RDF of sodium selenite in aqueous solution was calculated. The Se-O bond distance in the hydrated ion is 1.709 Å. The $O_w \cdots O_w$ distance in bulk water is 2.873 Å, outside of the bound oxygens the proximal $Se \cdots O_w$ distance is 3.87 Å. For the distal $Se \cdots O_w$ outside of the lone electron-pair the distance is 4.36 Å. The mean O···O distances are in the range between 2.83 and 2.86 Å. In combination with the Se-O distance and $Se \cdots O_w$ distance this gives an estimated $O_{SeO3} \cdots O_w$ distance of 2.85 Å. Using these assumptions, the angle ∠Se_O···O_w is 114°, thus between the expected values of 109.47 for a tetrahedral and 120.0 for a trigonal configuration around the water oxygens. This observation in correlation with the unusually broad distance distribution with a temperature factor of 0.048 $Å^2$, strongly indicates that the coordination is an equilibrium between 2- and 3-coordination around the oxygens through weak hydrogen bonding.

From the EXAFS studies, selenite Se-O bond distance is 1.701 Å for the selenite ion, 1.704 Å for the hydrogenselenate ion, $HSeO_3^-$, and 1.714 Å for selenous acid, H_2SeO_3, in aqueous solution. The commonly occurring elongation upon hydration seen in LAXS as compared to solid was not equally clear. The white-line maximum was determined to 12664.65 eV for the selenite ion. By studying the XANES spectra for the selenite ion, the hydrogenselenate ion and selenous acid there are substantial differences in the spectra, such as the hump with maximum around 126765 eV for the selenite ion, although the white line maxima are the same, Figure 7.

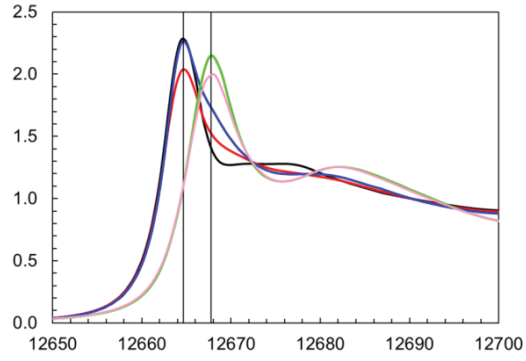

Figure 7. X-ray absorption near edge structure spectra (XANES) of sodium selenite (black), sodium hydrogenselenate (red), selenous acid (blue), sodium selenate (green) and sodium hydrogenselenate (pink) in aqueous solutions. The black vertical lines mark the "white" line energy.

DDIR analysis of the selenite showed an O-D stretch for the affected waters to be 2491± 2 cm^{-1} which corresponds to a molecular interaction energy of the water of ΔU_w=-45.2kJ mol^{-1}. This corresponds to a very weak structure maker as bulk water interactions are at 2509 cm^{-1}.

3.2.2 Selenate ion

The Se-O bond distance is 1.657 Å and the Se···O_w distance is 3.94 Å in the hydrated selenate ion. The O_w···O_w distance in bulk water is 2.861 Å as the O_{SeO4}···O_w and O_w···O_w distances were not separable, and the mean value is substantially shorter than the 2.89 Å often found for unaffected bulk water. This indicates that the O_{SeO4}···O_w distance is in the range 2.81-2.85 Å. The selenate ion is a structure maker (Gurney, 1953; Marcus, 2009) which was confirmed by the estimated O_{SeO4}···O_w distance and the results from the DDIR measurements. The complementary result for structure determination by EXAFS gave a Se-O bond distance of 1.643 Å. The distances determined by EXAFS are slightly shorter and more precisely determined. The Se-O distance found in selenate ion in water is of the same length as the comparable distance found in the solids of Na_2SeO_4•$5H_2O$, 1.644 Å and Na_2SeO_4, 1.646 Å, and of the same length as in $HSeO_4^-$ in aqueous solution, 1.642 Å. The XANES spectra Figure 7 show a white-line maximum at 12667.75 eV for the selenate

ion, and there are no discernible differences except a minor white-line intensity difference between the selenate and hydrogenselenate ions.

When the DDIR spectra were subjected to deconvolution, the peak maximum for the main hydration peak was at 2480±39 cm^{-1} although this covers the normal water peak at 2509 cm^{-1}.

3.3 Oxohalo anions

3.3.1 Hypochlorite ion

The structure parameters of the hydrated hypochlorite were determined by LAXS with a Cl-O bond distance of 1.662 Å and a chlorine to water oxygen, $Cl\cdots O_{aq,}$ distance of 3.25 Å. The hypochlorite coordinates 8 waters of which 5 are predominantly hydrogen bound to the chlorine atom and three to the oxygen. The water-water oxygen distance, $O_{aq}\cdots O_{aq}$ was not separable from the hypochlorite oxygen to water oxygen, $O\cdots O_{aq}$ distance and the peak maxima is a linear combination of these components at 3.046 Å. This unusually long distance is much weaker and longer that those found for the other oxochloro anions, and it is an indication that sodium hypochlorite may act as a hydrated melt rather than a hydrated aqueous solution.

3.3.2 Chlorite ion

The hydrated chlorite ion in aqueous solution has a Cl-O bond distance of 1.591 Å, as determined by LAXS, and 1.577 Å as determined by QMCF. If one accounts for thermal the broadening of the peaks there is no significant difference between the distances obtained by the two techniques. The $Cl\cdots O_{aq}$ distance is 3.882 and 3.783 Å using

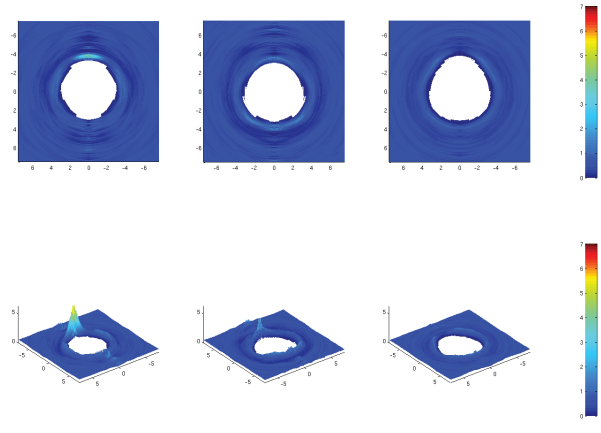

Figure 8. The chlorine-oxygen angular radial function analysis of chlorite (left), chlorate (middle) and perchlorate ions(right) from QMCF/MM simulation.

respective techniques. Further analysis of the peak using simulation data and separation in distal (below the chlorine plane with a normal vector defined by the axis) and proximal, above plane, distances there is an indication that there are two slightly different maxima comprising the $Cl\cdots O_{aq}$ peak. The mean $O_{aq}\cdots O_{aq}$ distance was determined by LAXS to 2.890 Å which is typical for that of unaffected bulk water of concentrated electrolyte solutions.

The two lone electron-pairs on the chlorite ion clearly dominate the interaction mechanism with the water for this weak structure breaker, as the ARD, Figure 8 left, show a significantly higher peak near the center of the symmetry axis on the lone pair side. Using hydrogen bond autocorrelation function S(t), Figure 9 top, it was shown that the hydrogen bond lifetime of the waters binding to the chlorine lone pairs were 0.239 ps and to the chlorite oxygens 0.415 ps. This means that the lone-pair water hydrogen bonding lasts 57.5 % of the corresponding oxygen hydrogen bond in the hydrated chlorite ion. This explains the difference in dynamic behavior as it enables a higher exchange rate at the chlorine lone electron-pair side. Mean residence time was 1.6 ps as compared to bulk water of 1.7 ps. This means that for chlorine the hydrogen bonds at the lone electron-pair side are about half as strong as those to the chlorite oxygen side.

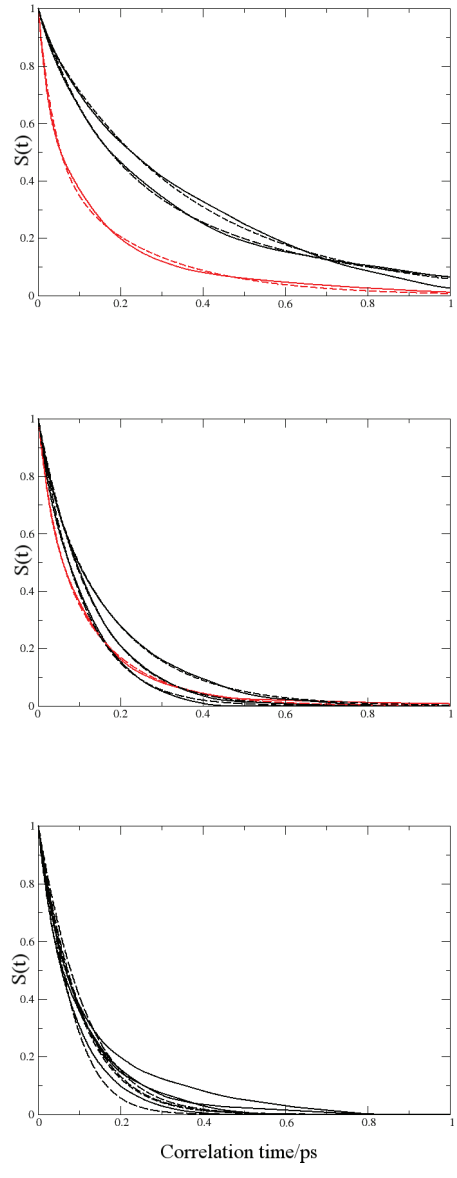

Figure 9. Contious hydrogen bond correlation function S(t) for chlorite(top), chlorate (middle) and perchlorate(bottom), red solid line depicts Cl···H-O bond ,black solid line O···H-O bond. The dashed lines are the corresponding fitted curves.

3.3.3 Chlorate ion

The hydrated chlorate ion in aqueous solution has a Cl-O bond distance of 1.501 and 1.487 Å using LAXS and QMCF data, respectively. This small difference is covered by the thermal distribution of the distances. The $Cl\cdots O_{aq}$ is 3.771 Å using LAXS and 3.960 Å using QMCF simulation. The distance for the simulation had an unusually high peak broadening with fwhh being almost 5 times that fwhh of the given for corresponding LAXS measurement. The oxygens of the chlorate ion have a distance to the water oxygens, $O\cdots O_{aq}$, of 3.021 and 2.93 Å as determined by LAXS and simulations, respectively. Again the distance distribution was much broader in the simulation than coresponding data from LAXS. The bulk water peak was at 2.889 Å. All structure factors found are given in Table 2 .

The hydrated chlorate ion has an apparent symmetric structure that is revealed as an asymmetric structure at closer inspection. The ARD show a minimum near the oxygens and a peak in the ARD oriented out from the hydration towards the bulk, Figure 8. The ARD shows a lower amount of structure as the distributions are more smeared out. This is in agreement with the chlorate ion being a structure breaker as shown in other studies (Marcus, 2009). For the chlorate ion the mean hydrogen bond lifetime, Figure 8 middle, for $O\cdots O_{aq}$ was 0.138 ps and for the chlorine lone electron-pair 0.150 ps showing an ability to form hydrogen bonds almost uniformly across the ion in aqueous solution. The molecular MRT of chlorate was determined to 2.05 ps, which is surprisingly long; this might be due to difficulties in determining a good cut-off radius for the MRT analysis as the peak might be convoluted by bulk water.

Table 2. Structure parameters for the oxochloro ions. *N* is the coordinating number as calculated from LAXS measurements, *d* is distance in Å, *b* is the temperature coefficients in $Å^2$, *l* the fwhh. The table's first four columns refer to LAXS data and the last from simulation data

Interaction	*N*	*d*	*b*	*l*	*D*	*l*
LAXS					QMCF/MD	
Hypochlorite ion						
Cl-O	1	1.662(6)	0.0058(8)	0.108(7)		
Cl···O_{aq}	5	3.251(5)	0.0127(5)	0.159(4)		
Cl(-O)···O_{aq}	3	3.85(2)	0.022(2)	0.21(1)		
O···O_{aq}/O_{aq}···O_{aq}	2	3.045(8)	0.025(2)	0.22(1)		
Na-O_{aq}	6	2.422(9)	0.0283(7)	0.24(1)		
Chlorite ion						
Cl-O	2	1.591(3)	0.0045(4)	0.069(7)	1.576(6)	0.067(1)
Cl···O_{aq}	6	3.881(6)	0.031(1)	0.25(1)	3.783(2)	0.92(4)
O···O_{aq}	2	3.045(8)	0.025(2)	0.23(1)	2.7875	0.454(2)
Na-O_{aq}	6	2.428(8)	0.0244(7)	0.221(3)		
O_{aq}···O_{aq}	2	2.890(2)	0.0210(3)	0.205(2)		
Chlorate ion						
Cl-O	3	1.501(2)	0.0030(4)	0.077(5)	1.487(0)	0.058(7)
Cl···O_{aq}	9	3.770(6)	0.0187(4)	0.193(3)	3.96041	0.93(1)
O···O_{aq}	2	3.021(4)	0.0251(6)	0.224(3)	2.9252(8)	0.75(5)
Na-O_{aq}	6	2.434(6)	0.0233(5)	0.216(3)		
O_{aq}···O_{aq}	2	2.889(2)	0.0198(3)	0.199(2)		
Perchlorate ion						
Cl-O	4	1.453(2)	0.0020(2)	0.063(3)	1.447(6)	0.064(0)
Cl···O_{aq}	12	3.757(6)	0.0306(9)	0.247(4)	4.076(X)	0.69(2)
O···O_{aq}	2	3.046(7)	0.0234(5)	0.216(3)	3.151(3)	0.70(4)
(H-)O···O_{aq}	4	2.693(6)	0.0109(5)	0.148(3)		
O_{aq}···O_{aq}	2	2.890(2)	0.0186(2)	0.192(2)		

3.3.4 Perchlorate ion

Investigations showed a distinct Cl-O distance within the perchlorate ion at 1.453 and 1.448 Å using LAXS and simulation, respectively, with an almost identical peek broadening. The perchlorate ion have also a much higher peak broadening for the simulation derived values than from LAXS measurements for the hydrated water oxygen distances with Cl···(H-)O_{aq} at 3.76 and 4.08 Å from LAXS and QMCF, respectively, having almost 3 times the fwhh in the simulation. The bulk water O_{aq}···O_{aq} distance was determined by LAXS at 2.890 Å. The structural parameters of the hydrated perchlorate ion from the LAXS and QMCF studies are given in Table 2.

The hydrated perchlorate ion shows a very typical symmetric behavior with a symmetric ARD with minima and maxima appearing in centro-symmetric waves out from the ion. In the perchlorate ion solution the mean hydrogen bond life time was 0.140 ps as given from the long component from double exponential fitting of $S_{HB}(t)$, Figure 9 bottom. The mean residence time of the hydration sphere was determined to 1.4 ps confirming it as a weak structure breaker.

Table 3. . Structure parameters for the bromate, iodate and periodate ions. *N* is the coordinating number as calculated from LAXS measurements, *d* is distance in Å, *b* is the temperature coefficients in Å^2, *l* the fwhh.

Interaction	*N*	*d*	*b*	*l*
Bromate ion				
Br-O	3	1.671(2)	0.0020(2)	0.063(6)
Br···O_{aq}	9	4.068(6)	0.0282(7)	0.237(3)
O···O_{aq}	2	2.987(8)	0.0257(6)	0.227(3)
Na-O_{aq}	6	2.434(6)	0.0233(5)	0.216(3)
O_{aq}···O_{aq}	2	2.890(2)	0.0200(3)	0.200(2)
Iodate ion				
I-O	3	1.829(5)	0.0056(4)	0.106(4)
I···O_{aq}	9	4.27(1)	0.0187(4)	0.193(3)
O···O_{aq}	2	3.013(4)	0.0258(6)	0.224(3)
Na-O_{aq}	6	2.432(6)	0.0251(5)	0.216(3)
O_{aq}···O_{aq}	2	2.890(2)	0.0200(2)	0.200(2)
Metaperiodate ion				
I-O	4	1.781(2)	0.0061(2)	0.110(3)
I···O_{aq}	12	4.243(4)	0.0259(6)	0.228(2)
O···O_{aq}	2	3.009(4)	0.0268(8)	0.232(3)
Na-O_{aq}	6	2.43(2)	0.029(3)	0.24(2)
O_{aq}···O_{aq}	2	2.890(2)	0.0199(2)	0.200(2)

3.3.5 Bromate, iodate and periodate ions

The structures of the the bromate, iodate and metaperiodate ions in aqueous solution were determined by LAXS and the structure parameters are summarized in Table 3. None of the ions studied showed any significant shift in the bulk water O_{aq}···O_{aq} distance, 2.89 Å. It was confirmed that in solid periodate there are two conformers, metaperiodate, IO_4^-, and ortoperiodate, IO_6^{5-}. In metaperiodate iodine bind oxygens in a tetrahedral configuration at a mean distance of 1.756 Å, Table S1 in Paper IV, with a narrow bond

distribution. In ortoperiodate the iodine binds to six oxygens and have a mean I-O distance of 1.886 Å with a broad distance distribution, Table S1 in Paper IV. This difference was not seen in aqueous solution independently of the source of periodate. The aqueous solution of metaperiodate had a I-O distance of 1.78 Å as determined by EXAFS showing that metaperiodate is predominating form in aqueous solution.

3.3.6 Summary

The oxohaloo anions showed little effect on the bulk water peak position of 2.89 Å with the exception of hypochlorite a 3.046 Å. Comparing simulation with LAXS, when applicable, showed significant broadening compared with the ion to water peaks in simulation. The ARD for the oxochloro anions studied showed a flat structure indicating a low amount of order in the systems. According to the determined MRT:s the structure maker to breaker for the oxohalo anions are from weakest to strongest structure breaker $ClO_2^- > ClO_3^- > ClO_4^-$

4 Discussion and Conclusion

4.1 Comparison Symmetric hydration of oxo anions

Previous studies of the sulphate ion (Vchirawongkwin *et al.*, 2007) and perchlorate (Lindqvist-Reis *et al.*, 1998) using LAXS, QMCF and DDIR have shown that these system have a symmetric hydration shell with one distance for $X\cdots O_{aq}$, 3.612 and 3.046 Å, respectively, where X is either S or Cl. It was also found that the selenate ion has only one $Se\cdots O_{aq}$ distance in the hydration shell of 3.94 Å. In Paper I it was shown that the exchange dynamics of the sulfate ion are symmetric with water migration to and from the hydration shell occurring in all directions, see Figure 10. In paper IV similar exchange effects are noticeable using the ARD plot of the simulated data on perchlorate ion. The selenate ion was only studied experimentally and therefore lacks dynamic information, and has as mentioned earlier a similar symmetric structure to both sulfate and perchlorate. This indicates that the hydration dynamics follow the symmetric pattern with equal exchange in all directions. The symmetric systems covered in this thesis had correspondingly high symmetry of the hydration both structurally and mechanistically. This of course confirms earlier studies on the anionic species and means that they make a good reference model.

4.2 Asymmetric hydration

The sulfite and selenite ions have two hydration distances from central atom to oxygens of hydrating water molecules in aqueous solution, 3.68 and 4.16 Å for the sulfite ion, and 3.87 and 4.36 Å for the selenite ion. For the chlorate ion the difference in the distances seen when one places a plane cutting through the centre of the chlorine atom and with a normal parallel with the axis of symmetry, is less than 0.03 Å, which explains why the distances are not differentiable in experiment. The asymmetry of the chlorate ion is best observed using ARD analysis where the localized minima can be observed. In contrast to the symmetric case the systems with one voxel occupied by a lone electron-pair instead of an oxygen has a mechanism that is quite different as shown by

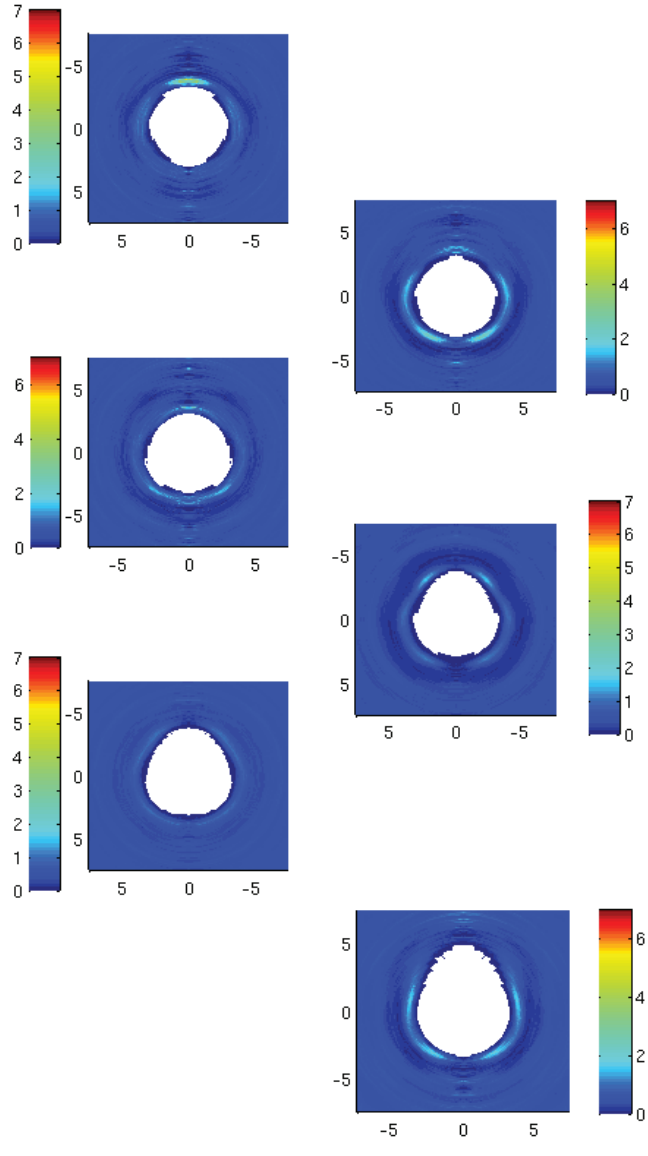

Figure 10. The ARD functions plotted for chlorite (top left), chlorite(middle left), perchlorate(bottom left), sulfite (top rigth), sulfate (middle right) and thiosulfate (bottom right).

performing angular radial distribution analysis and pathway analysis of the water molecules in the hydration sphere, see Figure 10. The results from the LAXS studies of the selenite ion show that it also exhibit two average distances for the hydration shell, which indicates an asymmetric hydration shell. There are indications in the similarities in structure data that suggest that selenite ion also has asymmetric lone electron-pair dominated water exchange dynamics.

In this thesis, I have shown that there is a lone electron-pair dominated hydration exchange dynamics between first shell water molecules and the surrounding bulk occurring for the sulfite ion as well as strong structural indications of the same mechanisms dominates for the hydrated selenite ion. With lone electron-pair dominated exchange, I mean that the hydrating water molecules in the first hydration shell can mostly transfer away from direct interactions with the ion, through movement along the axis and a narrow angle cone around it. This exchange happens when the hydrogen bonding to the ion is very weak with only transient weak interactions with the ion, while the interactions with neighbouring water molecules are mostly unaffected as compared to the bulk. In the case of the chlorite and chlorate ions, one can see that the interactions are affected by lone electron-pairs, but as both are weak structure breakers the already weak interactions with the hydrating water makes the effect much less pronounced. The asymmetry of the chlorite and chlorate ions can only be seen in the existence of more pronounced minima around the oxygens and are not as clear as from the structural parameters. The $S(t)$ of the chlorite ion clearly show a weaker hydrogen bonding at the chlorine site while the chlorate ion shows hydrogen bond life times that are much more symmetrical, and is in that respect a borderline case between asymmetric and symmetric hydration.

4.3 Coordination number

The coordination of the oxo-anions followed a periodic trend shown in Tables 1 and 2, and in the structurally determined coordination numbers of selenite and selenate ions. The oxohalo and oxosulfur anion hydrogen bind on average 3 water molecules on each oxygen. The selenite ion has a coordination can be regarded as an equilibrium between two- and three-coordination around each oxygen, and with approximately three water molecules coordinated to the selenium lone electron-pair, while the selenate ion hydrogen bind on average two water molecules. This trend of lowered coordination as one goes down in the periodic table continues for the oxoarseno anions and telluric acid as demonstrated recently (Mähler *et al.*, 2013). Considering size of the hydration

sphere and the ions this effect cannot be attributed to crowding effects but must rise from the distribution of the electron density in the ions.

4.4 Influences of oxidation states on substituted oxo-anions

One can see that in the case of the hydrated thiosulfate ion structure there is a low amount of hydrogen bonding occurring close to the terminal sulfur, while the oxygens form much stronger hydrogen bonds to water. This is the main contribution to the weakening of the first shell water-to-water bonding. In the case of the oxosulfur anions it is clear that the distribution of the electrons across the ion is what governs the interaction. The usefulness of oxidation state/number to assess the hydration behaviour is therefore limited.

4.5 Difference between symmetric and asymmetric hydration

Ions with symmetric hydration, has a first shell that both is structurally symmetric with regards to ion-water interaction regardless of orientation and the exchange dynamics of the water from the first shell to subsequent shells or bulk water is also independent of orientation in regards to the oxygen atoms. However, the asymmetric systems have structural differences and mechanically different exchange dynamics, with the intermediate state demonstrated by thiosulfate showing that the interaction strength based on local electron density seems to be the determining factor. As the localized electron density decreases, the lifetime and strength of the hydrogen bond diminishes as the electrostatic interactions become weaker and as the difference passes some threshold energy the mechanism of exchange changes from the symmetric equal exchange to localized exchange mechanics. In the latter case the hydration shell only exchange water with surrounding water at certain geometric configurations in regards to the symmetry axis of the oxyanion.

4.6 Structure breaker versus structure maker.

The structure maker *versus* the structure breaker properties have been thoroughly studied using macroscopic properties (Marcus, 1994, 2009). This study has added knowledge on the atomic level regarding the oxo anions. It is shown that the ions where hydrogen bonding was weak between hydrating water molecules and the ions (oxochloro anions) the hydrating water molecules have high mobility. There are in those cases a difficulty in discerning the boundaries of the hydration shell, as expected of structure breakers, whereas for those ions with stronger more lasting hydrogen bonds (oxosulfur anions)

one see a clear distinction between the hydration shell and the surrounding bulk water. This behaviour also enables the asymmetric behaviour in hydration to be clearly seen when the difference in localized electron density is sufficiently large as for the sulfite ion. The same structural behaviour is seen in the comparison of oxoseleno with sulfur anions. Therefore one can conclude that the weaker hydrogen bonding in combination with small difference in localized electron distribution over the ion means that the oxo anion behaves as a structure breaker, while stronger hydrogen bonding and large difference in localized electron densities have structural and mechanistically support as structure makers. As seen in Table 4 this would result in the following series based on MRT analysis from ions with structure making to structure breaking properties, left of water are structure makers and ions to the right are structure breakers: $PO_4^{3-} > SO_3^{2-} > SO_4^{2-} > ClO_3^- > H_2O > ClO_2^- > ClO_4^-$. Accounting for the short simulation time with regards to MRT analysis and the issues regarding spherical cut-off of asymmetrical interaction in ClO_3m SO_3^- and correlating with experimental structure data the series becomes $PO_4^{3-} > SO_3^{2-} > SO_4^{2-} > H_2O > ClO_2^- > ClO_3^- > ClO_4^-$ which follows the series using macroscopic properties of the solution as presented by Marcus (Marcus, 2009).

Table 4. *Summation of values obtained from MRT analysis in Papers I ,III and IV, $\tau_{0.5}$ is the mean residence time for t*=0.5 ps given in ps, S_{ex},is the sustainability coefficient. The $N_{ex0.5}$ and $N_{ex0.0}$ is the number of successful exchanges given t*=0.5 ps and t*=0.0 respectively.*

Hydrated ion	$\tau_{0.5}$	$N_{ex0.5}$	$N_{ex0.0}$	$1/S_{ex}$
Perchlorate	1.4	106	431	4.1
Sulfate	2.6	54	399	7.4
Phoshate	3.9	42	132	3.1
Chlorate	2.1	67	234	3.5
Sulfite	3.2	59	346	5.9
Chlorite	1.6	76	257	3.4
Bulk wate	1.7	24	269	11.2

4.7 Oxo-anion behavior contra anionic behavior of single ions

The oxo-anions displayed a delocalized electron behaviour not seen in simple ions. This delocalization, and the variations in the degree of localization in the species, gives rise to the complex behaviour of these oxo anions. This includes the interaction with an electron cloud on the asymmetric anions that is much weaker than the interactions of the oxygens compared to the more symmetrical systems with a higher degree of delocalization, giving these systems a uniform interaction with the hydrating waters. A notable exception to this is the hypochlorite ion, which from the LAXS studies it can be regarded that the chlorine and oxygen atoms act as independent units giving a coordination chemistry behaviour more similar to the atomic chloride ion while the oxygen behave an oxygen in any oxo anion. The oxo anions have complex binding structures that are dominated by weak hydrogen bonds while the atomic systems have easily identifiable hydrogen bonding.

5 Future interests

The mechanistic difference in water exchange mechanism for the hydration between the lone electron-pair dominated exchange and that of systems with fully occupied voxels could be of interest for further analysis, as it has profound effects on the solution properties. In addition, the investigation into the difference in hydration systems between the structure breakers and structure makers that is possible to study using the anionic systems could benefit from further studies. I believe that further combined studies with both experimental and computational methods are required to answer these problems, as the exchange rates are faster than current experimental methods allow for and as has been proven in earlier papers without the experimental groundwork it is easy to get non-physical artifacts in the computational work. Regarding the MRT analysis it is clear that more work is needed on the analysis algorithms to handle the complex interactions that oxo anions display.

References

Allen, F. H. (2002). The Cambridge Structural Database: a quarter of a million crystal structures and rising. *Acta Crystallographica Section B Structural Science* 58(3), 380–388.

Arunan, E., Desiraju, G. R., Klein, R. A., Sadlej, J., Scheiner, S., Alkorta, I., Clary, D. C., Crabtree, R. H., Dannenberg, J. J., Hobza, P., Kjaergaard, H. G., Legon, A. C., Mennucci, B. & Nesbitt, D. J. (2011). Definition of the hydrogen bond (IUPAC Recommendations 2011). *Pure and Applied Chemistry* 83(8), 1637–1641.

Belsky, A., Hellenbrandt, M., Karen, V. L. & Luksch, P. (2002). New developments in the Inorganic Crystal Structure Database (ICSD): accessibility in support of materials research and design. *Acta Crystallographica Section B Structural Science* 58(3), 364–369.

Bergerhoff, G. & Brown, I.D. (1987) in „Crystallographic Databases“, F.H. Allen et al. (Hrsg.) Chester, International Union of Crystallography,

Chandler, J. P. (1969). STEPIT: Finds local minima of a smooth function of several parameters (CPA 312). *Behavioral Science* 14, 81–82.

Cromer, D. T. (1967). Compton Scattering Factors for Spherically Symmetric Free Atoms. *The Journal of Chemical Physics* 47(6), 1892.

Cromer, D. T. (1969). Compton Scattering Factors for Aspherical Free Atoms. *The Journal of Chemical Physics* 50(11), 4857.

Frisch, M. J., Trucks, G. W., Schlegel, H. B., Scuseria, G. E., Robb, M. A., Cheeseman, J. R., Montgomery, J., Vreven, T., Kudin, K. N., Burant, J. C., Millam, J. M., Iyengar, S. S., Tomasi, J., Barone, V., Mennucci, B., Cossi, M., Scalmani, G., Rega, N., Petersson, G. A., Nakatsuji, H., Hada, M., Ehara, M., Toyota, K., Fukuda, R., Hasegawa, J., Ishida, M., Nakajima, T., Honda, Y., Kitao, O., Nakai, H., Klene, M., Li, X., Knox, J. E., Hratchian, H. P., Cross, J. B., Bakken, V., Adamo, C., Jaramillo, J., Gomperts, R., Stratmann, R. E., Yazyev, O., Austin, A. J., Cammi, R., Pomelli, C., Ochterski, J. W., Ayala, P. Y., Morokuma, K., Voth, G. A., Salvador, P., Dannenberg, J. J., Zakrzewski, V. G., Dapprich, S., Daniels, A. D., Strain, M. C., Farkas, O., Malick, D. K., Rabuck, A. D., Raghavachari, K., Foresman, J. B., Ortiz, J. V., Cui, Q., Baboul, A. G., Clifford, S., Cioslowski, J., Stefanov, B. B., Liu, G., Liashenko, A., Piskorz, P., Komaromi, I., Martin, R. L., Fox, D. J., Keith, T., Al-Laham, M. A., Peng, C. Y., Nanayakkara, A., Challacombe, M., Gill, P. M. W., Johnson, B., Chen, W., Wong, M. W., Gonzalez, C. & Pople, J. A.*Gaussian 03, Revision E.01*.

Gurney, R. W. (1953). *Ionic Processes In Solution* [online]. McGraw-Hill Book Company, Inc. Available from: http://archive.org/details/ionicprocessesin031465mbp. [Accessed 2013-12-09].

Jalilehvand, F. (2000). *Structure of hydrated ions and cyano complexes by X-absorption spectroscopy*. Diss. KTH. Available from: http://kth.diva-portal.org/smash/record.jsf?searchId=1&pid=diva2:8704. [Accessed 2014-05-01].

Johannson, G. & Sandström, M. (1973). *Chemica Scripta* 4, 195.

Kristiansson, O., Lindgren, J. & De Villepin, J. (1988). A quantitative infrared spectroscopic method for the study of the hydration of ions in aqueous solutions. *The Journal of Physical Chemistry* 92(9), 2680–2685.
Lindqvist-Reis, P., Muñoz-Páez, A., Díaz-Moreno, S., Pattanaik, S., Persson, I. & Sandström, M. (1998). The Structure of the Hydrated Gallium(III), Indium(III), and Chromium(III) Ions in Aqueous Solution. A Large Angle X-ray Scattering and EXAFS Study. *Inorganic Chemistry* 37(26), 6675–6683.
Marcus, Y. (1994). ViscosityB-coefficients, structural entropies and heat capacities, and the effects of ions on the structure of water. *Journal of Solution Chemistry* 23(7), 831–848.
Marcus, Y. (2009). Effect of Ions on the Structure of Water: Structure Making and Breaking. *Chemical Reviews* 109(3), 1346–1370.
Molund, M. & Persson, I. (1985). *Chemica Scripta* 25, 197.
Mähler, J., Persson, I. & Herbert, R. B. (2013). Hydration of arsenic oxyacid species. *Dalton Transactions* 42(5), 1364–1377.
Ohtaki, H. & Radnai, T. (1993). Structure and dynamics of hydrated ions. *Chemical Reviews* 93(3), 1157–1204.
Persson, I. (1984). *X-ray scattering on liquids, solutions,melts and nonchrystaline solids*.
Prince, E. (Ed.) (2006). *International Tables for Crystallography: Mathematical, physical and chemical tables* [online]. 1. ed. Chester, England: International Union of Crystallography. Available from: http://it.iucr.org/C/. [Accessed 2014-05-06].
Rode, B., Hofer, T., Randolf, B., Schwenk, C., Xenides, D. & Vchirawongkwin, V. (2006). Ab initio quantum mechanical charge field (QMCF) molecular dynamics: a QM/MM – MD procedure for accurate simulations of ions and complexes. *Theoretical Chemistry Accounts: Theory, Computation, and Modeling (Theoretica Chimica Acta)* 115(2), 77–85.
Rode, B. M. & Hofer, T. S. (2006). How to access structure and dynamics of solutions: The capabilities of computational methods (Special Topic Article). *Pure and Applied Chemistry* 78(3), 525–539.
Smiechowski, M.*YANUZ.AB*. Technical University of Gdansk, Gdansk, Poland.
Stangret, J. & Gampe, T. (1999). Hydration Sphere of Tetrabutylammonium Cation. FTIR Studies of HDO Spectra. *The Journal of Physical Chemistry B* 103(18), 3778–3783.
Stangret, J. & Gampe, T. (2002). Ionic Hydration Behavior Derived from Infrared Spectra in HDO. *The Journal of Physical Chemistry A* 106(21), 5393–5402.
Trinapakul, M., Kritayakornupong, C., Tongraar, A. & Vchirawongkwin, V. (2013). Active site of the solvated thiosulfate ion characterized by hydration structures and dynamics. *Dalton Transactions* 42(30), 10807–10817.
Vchirawongkwin, V., Rode, B. M. & Persson, I. (2007). Structure and Dynamics of Sulfate Ion in Aqueous SolutionAn ab initio QMCF MD Simulation and Large Angle X-ray Scattering Study. *The Journal of Physical Chemistry B* 111(16), 4150–4155.

Acknowledgements

At this point, I would like to thank some of the individuals whom have influenced me and have had great impact on the process of my thesis.

First, I would like to thank my supervisor Ingmar Persson, who have taught me all I know of inorganic chemistry and always been prepared to help with experiments and endured my somewhat rough text draft and helped me turn them into readable articles. The second acknowledgement I wish to give is to Mats Petterson for always being there, whether it was in giving me a ride to the hospital or giving me scientific advice your help has been invaluable. Jonas Söderberg has also been a solid rock with both needful distractions and scientific discussions thank you for the input and for always taking the time to listen, may the MatLab always be with you. My wife Sandra has been invaluable support in my writing process and still is the sun in my life, your warm and loving nature inspires me. To assistant professor Thomas Hofer, professor Bernd M. Rode and the department of theoretical chemistry in Innsbruck for always having a warm hospitality and for hosting the simulations. Thomas I will miss both our scientific discussions and our gaming discussions, may you always find the elder scrolls you need. Gunnar Almkvist, our discussions on scientific data and your encouragements and kindness have always been helpful. Daniel Lundberg for making the illustration for the inside cover art for the in Dalton transactions vol 43, number 17. Many colleagues have been very helpful and been good friends during my time at the department of chemistry such as Kai Wilkinson, always a good friend to talk to, you got me started in the wonderful hobby of miniature crafting, it has helped calm me many stressful times. Johan Mähler, while we might not agree on all philosophical discussions we have had, I feel that they have been rewarding and fun. Shahin Norbakhsh you were always willing provide conversational distraction when I needed a break, Gustav Nestor and Pierre, I enjoyed the conversations on kids, life and the universe in large that the parties and break

room provided. Bernt Andersson, always reliable and willing to help when I did my assistant teaching in the lab. Sonja Jansson, thank you for always keeping the door open. Vadim for running the department excellently, we have had many interesting talks in the lunchroom, on chemistry, history and more. Gulaim Seisenbaeva for the use and assistance concerning the IR equipment at the department and to all the rest of my colleagues it has been a pleasure working with you and you have all contributed to make my stay at the department wonderful. To my friends outside of work, Magda, Daniel the rest of the the roleplaying gang there have been many fun filled sessions over the years. My long-time friend Daniel Persson, we have gotten lost together quite often and always it has been a wonderful experience, be it scouting, politics, or MTG, you have always been a solid friend thank you

. My family I will thank in Swedish.

Till min familj Pappa du har alltid varit ett stort stöd och alltid villig att hjälpa till med vilken galen idé, hobby eller annat jag velat göra. Mamma du har fått stå ut med mina och pappas diskussioner i många år och alltid varit en trygghet för mig. Anki för att alla behöver någon att prata av sig med. Kenneth för att du alltid tror på att jag kan och kommer att lyckas. Kicki och Lasse de bästa svärföräldrar man kan ha. Ni ställer alltid upp och hjälper alltid till, tack för att ni finns.

Finally I would also like to thank the Swedish Research Council and the Austrian Science Foundation which have financed this project and the MAX Laboratory at Lund University, Sweden for granting beam time at the I 8-11for the XAS experiments as well as to Stanford Synchrotron Radiation Lightsource (SSRL),Stanford university, Stanford, California, USA for allocated beam time at the 4-1 beamline